

---

## Technical Note

---

# INTRODUCTION TO MESHLESS LOCAL PETROV-GALERKIN METHOD

**Pamuda Pudjisuryadi**

Lecturer, Department of Civil Engineering, Faculty of Civil Engineering and Planning  
Petra Christian University, Surabaya

### Catatan Redaksi:

Makalah ini adalah seri kedua dari dua yang membahas *Meshless Numerical Analysis Method*, suatu metode analisa numerik yang berkembang dengan pesat sebagai alternatif metode elemen hingga (*Finite Element Method*). Makalah seri pertama yang mengenalkan *Moving Least-Squares Approximation* telah dimuat dalam Dimensi Teknik Sipil, Vol 4., No. 1, Maret 2002.

### INTRODUCTION

In recent years, meshless methods have been developed as alternative numerical approaches in efforts to eliminate known drawbacks of the Finite Element Method (FEM). The main objective in developing meshless methods was to eliminate, or at least reduce, the difficulty of meshing and remeshing of complex structural elements. The nature of various approximation functions employed by meshless methods allows the definition of problem domains by simply adding or deleting nodes where desired. Nodal connectivity to form an element as in FEM method is not needed, only nodal coordinates and their domain of influence (DOI) are necessary to discretize the problem domain. Meshless methods may also reduce other problems associated with the FEM, such as solution degradation due to locking and severe element distortion [1].

There are several meshless methods under current development, including the Element-Free Galerkin (EFG) method proposed by Belytschko et al. [2], the Reproducing Kernel Particle Method (RKPM) proposed by Liu et al. [3], Smooth Particle Hydrodynamics (SPH) method proposed by Gingold and Monaghan [4]. The major difference in these meshless methods is in the choice of interpolation techniques they use. The above meshless method are meshless only from the point of view of the interpolation of the field variables, as compared to the FEM.

These meshless methods still use background cells to integrate the global Galerkin weak form.

Recently, another meshless method called Meshless Local Petrov-Galerkin (MLPG) has been developed [1]. This method is believed to have a good future due to its generality in choosing the form of test and trial functions and also that it is similar to the well established EFG method. Atluri et al. [1] proposed a new integration method in a local domain, based on a Local Symmetric Weak Form (LSWF). Therefore, the MLPG method is a truly meshless method, and all other meshless methods can be derived from it, as special cases, if trial and test functions and the integration method are chosen appropriately

### MESHLESS LOCAL PETROV-GALERKIN (MLPG) METHOD

For a two-dimensional linear, elastic boundary value problem in a global domain  $\Omega$ , bounded by  $\Gamma$  (Fig. 1), the force equilibrium equation can be written as:

$$\sigma_{ij,j} + b_i = 0 \quad \text{in } \Omega \quad (1)$$

where  $\sigma_{ij}$  is the stress tensor,  $b_i$  are the body forces, and  $\sigma_{ij,j}$  indicates the partial derivative of  $\sigma_{ij}$  with respect to coordinate direction  $x_j$ . Additionally, the boundary conditions may be written, respectively, as:

$$u_i = \bar{u}_i \quad \text{at } \Gamma_u \quad (2)$$

$$\sigma_{ij} n_j = \bar{t}_i \quad \text{at } \Gamma_t \quad (3)$$

---

Note: Discussion is expected before November, 1<sup>st</sup> 2002. The proper discussion will be published in "Dimensi Teknik Sipil" volume 5 number 1 Maret 2003.

where  $u_i$  is  $i^{\text{th}}$  component of displacement,  $\bar{u}_i$  and  $\bar{t}_i$  are prescribed displacements and tractions that are applied on boundary segments  $\Gamma_u$  and  $\Gamma_t$ , respectively, and  $n_j$  is the unit vector that is locally outward normal to the boundary. A generalized local weak form of the governing differential equation and the boundary conditions, over a local sub-domain  $\Omega_{te}^I \in \Omega$ , as shown in Figure 1, can be written as [1]:

$$\int_{\Omega_{te}^I} (\sigma_{ij,j} + b_i) v_i d\Omega - \alpha \int_{\Gamma_{su}^I} (u_i - \bar{u}_i) v_i d\Gamma = 0 \quad (4)$$

where  $\Gamma_{su}^I$  is the intersection of  $\Gamma_u$  and the boundary  $\partial\Omega_{te}^I$  of  $\Omega_{te}^I$ ,  $v_i$  is a test function that can be chosen with some degree of flexibility, and  $\alpha$  is a penalty parameter that sets the degree of influence of the second term in (4) with respect to the first term. The definitions of the various regions and boundaries relevant to the formulation of the MLPG method are clearly illustrated in Figure 2.

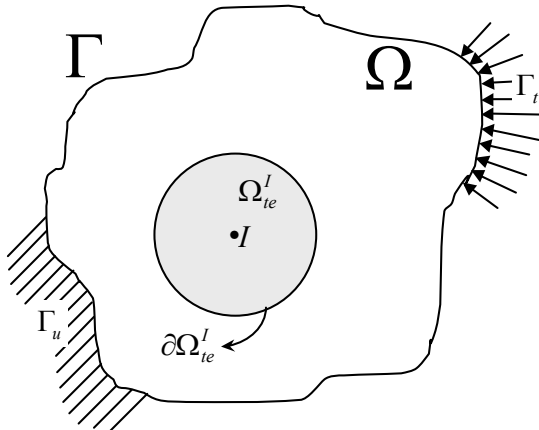


Figure 1. A schematic representation of the sub-domain  $\Omega_{te}^I$ , with node  $I$  as its center and with boundary  $\partial\Omega_{te}^I$ . The global domain is  $\Omega$  with a global boundary  $\Gamma$ , where displacement are prescribed on  $\Gamma_u$  and tractions are prescribed on  $\Gamma_t$ .

Further, if integration by parts and the divergence theorem are applied to the first term of Equation 4, the equation can be expressed as follows:

$$\int_{\partial\Omega_{te}^I} \sigma_{ij} n_j v_i d\Gamma - \int_{\Omega_{te}^I} \sigma_{ij} v_{i,j} d\Omega + \int_{\Omega_{te}^I} b_i v_i d\Omega - \alpha \int_{\Gamma_{su}^I} (u_i - \bar{u}_i) v_i d\Gamma = 0 \quad (5)$$

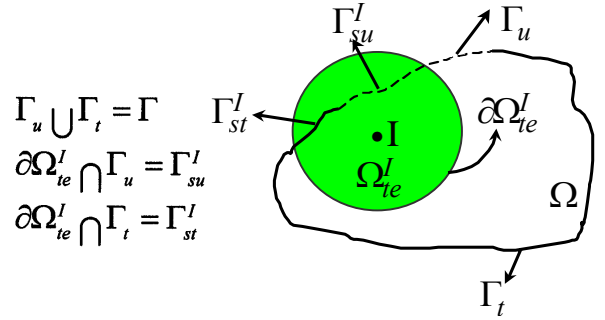


Figure 2. Important definitions if the domain of the test function  $\Omega_{te}^I$  intersects the global boundary  $\Gamma$ . The intersection of  $\Omega_{te}^I$  and  $\Gamma_u$  is defined as  $\Gamma_{su}^I$ , while its intersection with  $\Gamma_t$  is defined as  $\Gamma_{st}^I$ .

Noting that test function  $v_i = 0$  on  $\partial\Omega_{te}^I$  except if  $\partial\Omega_{te}^I$  intersects a global boundary  $\Gamma$ , Equation 5 can be rewritten as:

$$\int_{\Gamma_{su}^I} \sigma_{ij} n_j v_i d\Gamma + \int_{\Gamma_{st}^I} \sigma_{ij} n_j v_i d\Gamma - \int_{\Omega_{te}^I} \sigma_{ij} v_{i,j} d\Omega + \int_{\Omega_{te}^I} b_i v_i d\Omega - \alpha \int_{\Gamma_{su}^I} (u_i - \bar{u}_i) v_i d\Gamma = 0 \quad (6)$$

Finally, Equation 6 can be re-written in the following form (known as the local symmetric weak form):

$$\int_{\Omega_{te}^I} \sigma_{ij} v_{i,j} d\Omega + \alpha \int_{\Gamma_{su}^I} u_i v_i d\Gamma - \int_{\Gamma_{su}^I} t_i v_i d\Gamma = \int_{\Gamma_{st}^I} \bar{t}_i v_i d\Gamma + \alpha \int_{\Gamma_{su}^I} \bar{u}_i v_i d\Gamma + \int_{\Omega_{te}^I} b_i v_i d\Omega \quad (7)$$

where  $\Gamma_{st}^I$  is the intersection of  $\Gamma_t$  and the boundary  $\partial\Omega_{te}^I$ , and  $t_i = \sigma_{ij} n_j$ . Equation 7 leads to the  $I^{\text{th}}$  row of the global stiffness matrix. The  $J^{\text{th}}$  columns of the stiffness matrix correspond to all nodes whose domains of influence  $\Omega_{tr}^J$  intersect with the  $I^{\text{th}}$  test function's sub-domain  $\Omega_{te}^I$ , as shown in Figure 3.

Further, it can be shown if the radius of  $\Omega_{tr}^J$  and  $\Omega_{te}^I$  for each  $I$  and  $J$  are equal, and if  $u_i$  and  $v_i$  are the same for each  $I$  and  $J$ , then the stiffness matrix will be symmetric. In this study, the test function  $v_i$  is equal to zero at  $\partial\Omega_{te}^I$  except if  $\partial\Omega_{te}^I$  intersects the global boundary  $\Gamma$ , and the test function  $v_i$  is any function that is sufficiently well-behaved and integrable [5]. This means that the test function can take any shapes such as circular, ellipse, rectangular, polygonal, etc., as long as the above criterions are met.

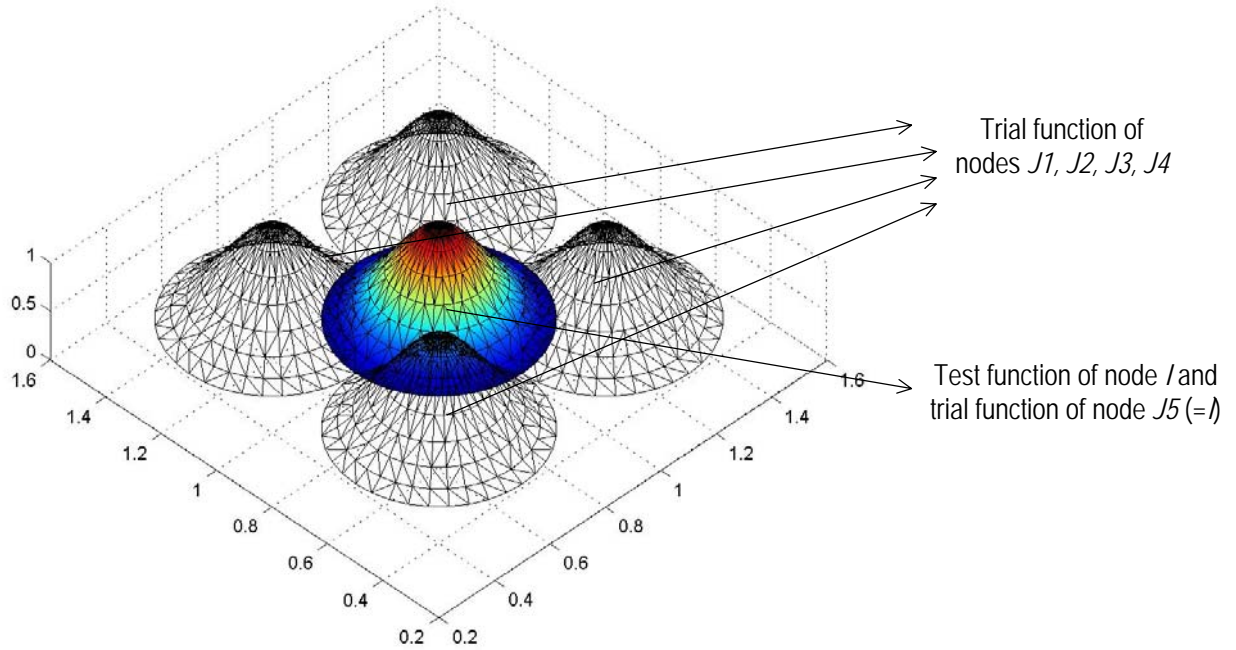


Figure 3. Intersections of test function and trial functions which leads to non-zero components in the  $I^{\text{th}}$  row of stiffness matrix. In the above figure, the  $I^{\text{th}}$  row of the stiffness matrix will have 10 non-zero components in a 2D elastostatic analysis.

To obtain the discrete equations from the MLPG formulation (7), the trial function  $u_i$  and test function  $v_i$  are defined as follows:

$$u_i(x) = \sum_{J=1}^N \phi^J(x) \hat{u}_i^J, \text{ and} \quad (8a)$$

$$v_i(x) = \sum_{I=1}^N \psi^I(x) \hat{v}_i^I \quad (8b)$$

where  $\phi^J(x)$  and  $\psi^I(x)$  are the nodal shape functions for the trial and test functions, respectively, and are centered at nodes  $J$  and  $I$ , respectively. The  $\phi^J(x)$  are constructed from Moving Least-Square (MLS) approximation functions and the  $\psi^I(x)$  are chosen as the weight functions used in MLS approximation at node  $I$ . Thus each nodal sub-domain is circular in shape. Typically, trial functions decrease smoothly to zero at the support boundaries, forming a bell-like shape in 2D domains (see Figure 3). In typical meshless interpolations,  $\hat{u}_i^J$  are referred to fictitious nodal values since they have no real physical meaning. Due to the nature of MLS approximation functions, which are not necessarily equal to unity at its corresponding node and equal to zero at their neighboring nodes, the nodal degrees of freedom in MLS based methods do not correspond to actual displacements at the nodes.

Substituting Equation 8 into Equation 7 and factoring  $\hat{v}_i^I$  (because it appears in each term of Equation 6, and also since it can be chosen arbitrarily) out of the equation, the discrete form of the MLPG formulation can be expressed as follows:

$$\sum_{J=1}^N \int_{\Omega_{te}^J} (B_v^J)^T DB^J \hat{u}^J d\Omega + \alpha \sum_{J=1}^N \int_{\Gamma_{su}^J} V^J \phi^J \hat{u}^J d\Gamma - \sum_{J=1}^N \int_{\Gamma_{su}^J} V^J NDB^J \hat{u}^J d\Gamma \quad (9)$$

$$= \int_{\Gamma_{su}^I} V^I \bar{u} d\Gamma + \alpha \int_{\Gamma_{su}^I} V^I \bar{u} d\Gamma + \int_{\Omega_{te}^I} V^I b d\Omega$$

where in two-dimensional space,

$$B_v^I = \begin{bmatrix} \psi_{,1}^I & 0 \\ 0 & \psi_{,2}^I \\ \psi_{,2}^I & \psi_{,1}^I \end{bmatrix}, B^J = \begin{bmatrix} \phi_{,1}^J & 0 \\ 0 & \phi_{,2}^J \\ \phi_{,2}^J & \phi_{,1}^J \end{bmatrix}, N = \begin{bmatrix} n_1 & 0 & n_2 \\ 0 & n_2 & n_1 \end{bmatrix}$$

$$V^I = \begin{bmatrix} \psi^I & 0 \\ 0 & \psi^I \end{bmatrix}, \hat{u}^J = \begin{Bmatrix} \hat{u}_1^J \\ \hat{u}_2^J \end{Bmatrix}, D = \frac{\bar{E}}{1-\bar{\nu}^2} \begin{bmatrix} 1 & \bar{\nu} & 0 \\ \bar{\nu} & 1 & 0 \\ 0 & 0 & \frac{1-\bar{\nu}}{2} \end{bmatrix}$$

and

$$\bar{E} = \begin{cases} E & \text{for plane stress} \\ E/(1-\nu^2) & \text{for plane strain} \end{cases} \text{ and } \bar{\nu} = \begin{cases} \nu & \text{for plane stress} \\ \nu/(1-\nu) & \text{for plane strain} \end{cases}$$

Further, Equation 7 can be written in a more compact form which we may already be familiar with, namely:

$$\sum_{J=1}^N K_{IJ} \hat{u}^J = f_I \quad (10)$$

where

$$K_{IJ} = \int_{\Omega_{te}^I} (B^I)^T DB^J d\Omega + \alpha \int_{\Gamma_{su}^I} V^I \phi^J d\Gamma - \int_{\Gamma_{su}^I} V^I NDB^J d\Gamma \quad (11)$$

$$f_I = \int_{\Gamma_{st}^I} V^I \bar{t} d\Gamma + \alpha \int_{\Gamma_{su}^I} V^I \bar{u} d\Gamma + \int_{\Omega_{te}^I} V^I b d\Omega$$

In the MLPG method, the usual assembly process, mapping non-zero components of local stiffness matrices into the global stiffness matrix based on the equation number of each degree of freedom, is not required to form the global stiffness matrix. In the MLPG method each local weak form (examining only one test function and the trial functions whose domains intersect with its domain) results in two rows (for two dimensional problems) of non-zero components of the global stiffness matrix. Theoretically, as long as the union of all local sub-domains  $\Omega_{te}^I$  covers the global domain, the equilibrium equation and the boundary conditions will be satisfied in the entire global domain  $\Omega$  and along its boundary  $\Gamma$  [1]. Solving Equation 10, the fictitious nodal displacement values  $\hat{u}^J$  at every node J can be obtained. Approximate solution can be obtained from Equation 8a, and by taking the derivative of this approximate solution and applying an appropriate stress-strain relationship (the Hooke's Law), the strain and the stress can be obtained.

### NUMERICAL EXAMPLES

Numerical examples are presented in this section to verify the method. A cantilever beam subjected concentrated load on its free end (Figure 4) will be analyzed with MLPG method using linear and quadratic basis functions in forming the MLS approximation and Gaussian Weight function [1] with circular domain as the test functions [6]. Uniform nodal distributions are used in this examples (6x4, 11x7 and 21x13). Domain of influence for trial function and radius of circular domain for test function of each node are chosen to be 3 times the nodal spacing.  $L_2$ Norm of displacement error  $\|e^u\|$  and relative  $L_2$ Norm of displacement error  $\|rel - e^u\|$  (after normalized with  $L_2$ Norm of exact displacement) over the entire problem domain are presented in Table 1. These two error measure are computed as followings :

$$\|e^u\| = \sqrt{\int_{\Omega} \{(u_{app} - u_{ex})^2 + (v_{app} - v_{ex})^2\} d\Omega} \quad (12)$$

$$\|rel - e^u\| = \frac{\|e^u\|}{\sqrt{\int_{\Omega} (u_{ex}^2 + v_{ex}^2) d\Omega}} \quad (13)$$

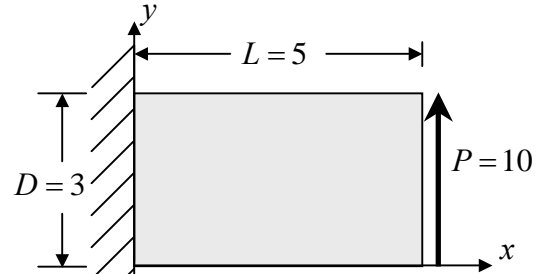


Figure 4. The Cantilever Beam Test

The analytical solution for the cantilever beam problem is given by Timoshenko [7] in this equation :

$$u = -\frac{P}{6EI} (y - \frac{D}{2}) [3x(2L - x) + (2 + \nu)y(y - D)] \quad (14)$$

$$v = \frac{P}{6EI} [x^2(3L - x) + 3\nu(L - x)(y - \frac{D}{2})^2 + \frac{4 + 5\nu}{4} D^2 x]$$

$$\sigma_{xx} = -\frac{P}{I} (L - x)(y - \frac{D}{2}) ; \sigma_{yy} = 0 ; \tau_{xy} = -\frac{Py}{2I} (y - D)$$

It can be seen from Table 1 that using more nodes to discretize the problem domain and increasing the basis function order used for constructing MLS approximation, improve the results.

Table 1. Results of cantilever beam test using DOI and radius of circular subdomain equal to 3 times of the uniform nodal spacing.

Basis Function	Linear	Quadratic		
	$\ e^u\ $	$\ rel - e^u\ $ %	$\ e^u\ $	$\ rel - e^u\ $ %
Nodal Distribution				
6x4 (1.00 unit spacing)	3.63x10 <sup>-2</sup>	7.80	1.71x10 <sup>-2</sup>	3.68
11x7 (0.50 unit spacing)	1.17x10 <sup>-2</sup>	2.50	2.64x10 <sup>-3</sup>	0.57
21x13 (0.25 unit spacing)	2.73x10 <sup>-3</sup>	0.59	7.15x10 <sup>-4</sup>	0.15

### SUMMARY

Some important features in MLPG are emphasized in this section. In MLPG method, data needed for problem discretization are nodal coordinates and their corresponding domain of influence. No nodal connectivity to form elements is necessary. In general, test functions and trial functions used in MLPG can be different which can lead to unsymmetrical stiffness matrix. Due to the nature of Moving

Least-Square shape function used in MLPG, that the value at corresponding node is not equal to 1 unit and zero at all other nodes, the degrees of freedom solved by MLPG formulation are not the real nodal values, they are fictitious. Real nodal values (and also other values at any locations in the problem domain) can be obtained by employing the MLS approximation with already known fictitious nodal values  $\hat{u}^J$ . It is believed that the accuracy of solution by MLPG method which employs smooth approximation (MLS) is good.

## REFERENCES

1. Atluri, S.N., Kim, H.G., Cho, J.Y. A critical assessment of the truly Meshless Local Petrov-Galerkin (MLPG), and Local Boundary Integral Equation (LBIE) methods. *Computational Mechanics* vol. 24, 1999, pp. 348-372.
2. Belytschko, T., Lu, Y.Y., Gu, L. Element-free Galerkin methods. *International Journal for Numerical Methods in Engineering* vol. 37, 1994, pp. 229-256.
3. Liu, W.K., Jun, S., Zhang, Y.F. Reproducing kernel particle methods. *International Journal for Numerical Methods in Fluids* vol .20, 1995, pp. 1081-1106.
4. Gingold, R.A., Monaghan, J.J. Smoothed particle hydrodynamics: theory and application to non-spherical stars. *Mon. Not. Roy. Astron. Soc.* vol. 181, 1977, pp. 375-389.
5. Becker, E.B., Carey, G.F., Oden, J.T. *Finite Element: An Introduction*, Volume I. New Jersey: Prentice-Hall, Inc., 1981.
6. Barry, W.J., Pannachet, T. Large deformation analysis of 2D elastic solids by the meshless local Petrov-Galerkin method. *AIT Thesis*, Bangkok, 2000.
7. Timoshenko, S.P., Goodier, J.N. *Theory of Elasticity – Third Edition*, McGraw-Hill Inc., U.S.A., 1987.